

6-7 days ahead of the projected landfall. However, the current RAT GUI can only be used once the hurricane enters the Gulf of Mexico and can be operational typically 2-3 days ahead of the landfall. Once an advisory is issued at the NHC, the RAT GUI operates in an autonomous mode extracting key data from the advisory, and then comparing those with the synthetic storms in the database and then displaying key results such as extent and height of storm surge with hydrographs in Google Earth. The operation repeats itself once a new advisory is issued at the NHC website.

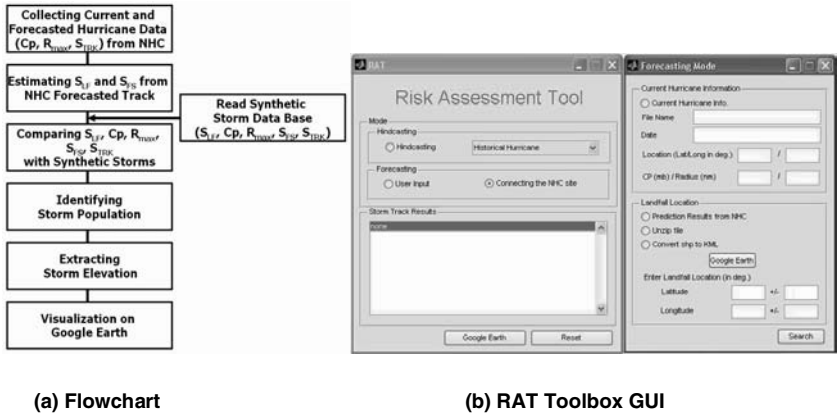


Figure 2. Real time RAT operation (a) Flowchart and (b) RAT GUI

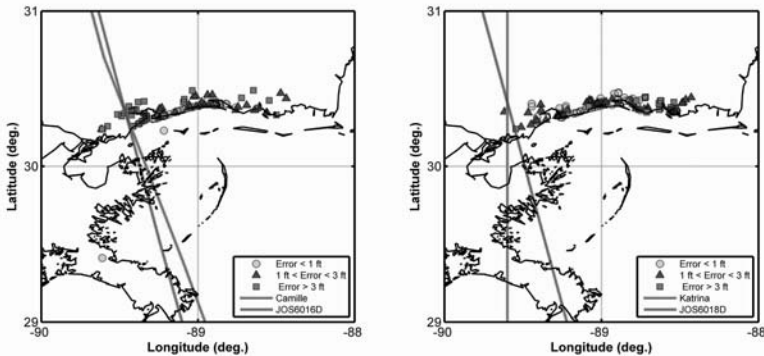
RESULTS

Model Validation

For validation, model results were compared with the observed High Water Marks (HWMs) from historical hurricanes including hurricanes Camille (1969) and Katrina (2005). These were selected as they made landfall close to Mississippi coast. As mentioned earlier, three parameters (i.e., S_{LF} , C_p , and R_{max}) were used as input to the RAT GUI. These three input parameters were extracted from the Best Track Information available at the NHC archived database. The RAT toolbox was able to quickly identify the best matching synthetic storms, which was JOS6016D for hurricane Camille and JOS6018D for hurricane Katrina stored in the database. Table 2 shows the input parameters to the RAT GUI and results of the matching synthetic storms for hurricane Camille and Katrina. Figure 3 shows the tracks for Hurricane Camille and Katrina with the best matching synthetic storms. The comparison of observed HWMs and model simulation results are also shown in Figure 3.

Table 2. Input values of hurricane parameters (landfall location and C_p and R_{max} for Hurricane Camille and Katrina and result of the best matching synthetic storms.

Input Parameters				Results			
Name	Landfall (lat/lon, °)	C_p (mb)	R_{max} (nm)	Name	Landfall (lat/lon, °)	C_p (mb)	R_{max} (nm)
Camille	30.3/-89.2	905	8	JOS6016D	30.1/-89.4	909	7.3
Katrina	29.3/-89.6	905	20	JOS6018D	29.9/-89.4	910	14.5



(a) Hurricane Camille

(b) Hurricane Katrina

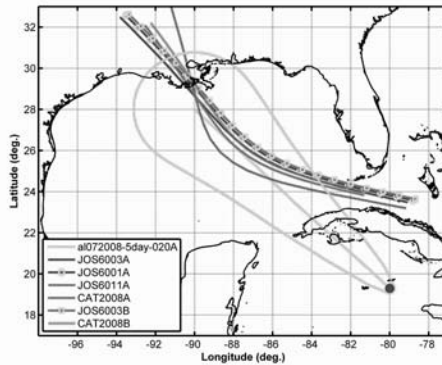
Figure 3. Track of Hurricane Camille and Katrina and the best matching synthetic storms (JOS6016D for Camille and JOS6018D for Katrina). The symbols show the HWM locations and their comparison with simulated results. Green dots show that the errors between observed and simulated HWM are less than 1 ft.

The comparison results with observed HWMs show that the RAT performs satisfactorily in hindcasting historical storms. The correlation between observed and modeled high water marks were reasonable ($R^2=0.81$ for both Katrina and Camille).

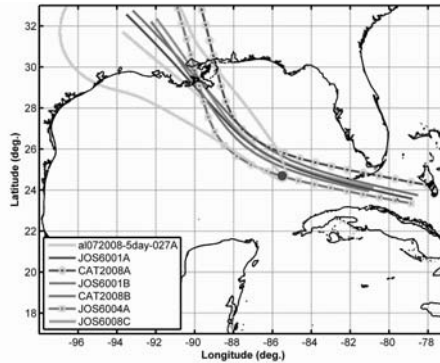
Model Application to Mississippi Coast

To demonstrate how the RAT toolbox performs in real time, advisory data issued during hurricane Gustav (August 29-31, 2008) were used. Two advisory data sets (al072008-5day-020A, and al072008-5day-027A; herein, referred as advisory numbers 20 and 27) were chosen. Each data set had the projected hurricane track along with current storm location, C_p and R_{max} values. Figure 4 shows the NHC forecasted Hurricane Gustav tracks and cone of uncertainty for advisory numbers 20 and 27. Figure 4 also shows the best matching synthetic storms with

highest Storm Similarity Index (SSI) values. It can be seen that for the NHC advisory number 20, synthetic storm JOS6003A had the highest SSI (0.84), whereas, for the advisory number 27, the SSI was updated and synthetic storm JOS6001A was found to be the best matching synthetic storm for the current Hurricane Gustav. Table 3 summarizes the results identifying the group of storms with high SSI values for these two advisories. Note that, due to significant changes in the C_p values from advisory number 20 to 27 (980 mb reduced to 958 mb), a new set of synthetic storms were identified by the RAT toolbox. For validation, the model results for advisory number 27 data were then compared with the observed HWMs (Figure 5). In general, the model surge elevations extracted from JOS6001A storm are in a reasonable agreement with the observed HWM(s). The lower correlation results for Gustav might occur for two reasons, (1) hurricane Gustav made landfall in the Louisiana coast and (2) the current database of the RAT is impaired with a storm population that concentrates only on the Mississippi coast. Nevertheless, even with the limitations of the current database, the application of the RAT Toolbox is promising. Figure 6 shows the forecasting results for Advisory number 27 displayed on the Google Earth.



(a) Advisory Number 20 and synthetic storm tracks



(b) Advisory Number 27 and synthetic storm tracks

Figure 4. Forecasted Hurricane Gustav tracks (Advisory Number 20 and 27) and synthetic storm tracks having the high SSI values. The blue dots (o) indicate the current hurricane location and the Green line shows the cone of uncertainty.

Table 3. Advisory forecast data from Hurricane Gustav. These data were used in the RAT GUI in forecasting mode.

Advisory Number	a1072008_5day_020A		a1072008_5day_027A	
Date	08/30/00:00		08/31/12:00	
Location (Lat/Long; °)	19.3/-80.0		29.1/-90.4	
Current C_p (mb)	980		958	
Current R_{max} (nm)	20		15	
Landfall Location (Lat/Long; °)	29.1/-91.0		29.1/-90.4	
Results	Synthetic Storm	SSI	Synthetic Storm	SSI
	JOS6003A	0.84	JOS6001A	0.82
	JOS6001A	0.80	CAT2008A	0.78
	JOS6011A	0.78	JOS6001B	0.73
	CAT2008A	0.77	CAT2008B	0.72
	JOS6003B	0.75	JOS6004A	0.71
	CAT2008B	0.71	CAT2008C	0.63

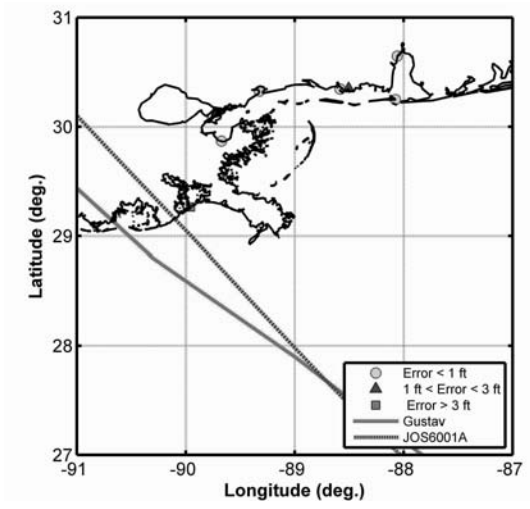


Figure 5. Track of Hurricane Gustav (in Red) and the best matching synthetic storm JOS6001A (in Blue). Green dots show the observed HWMs with errors less than 1 ft.

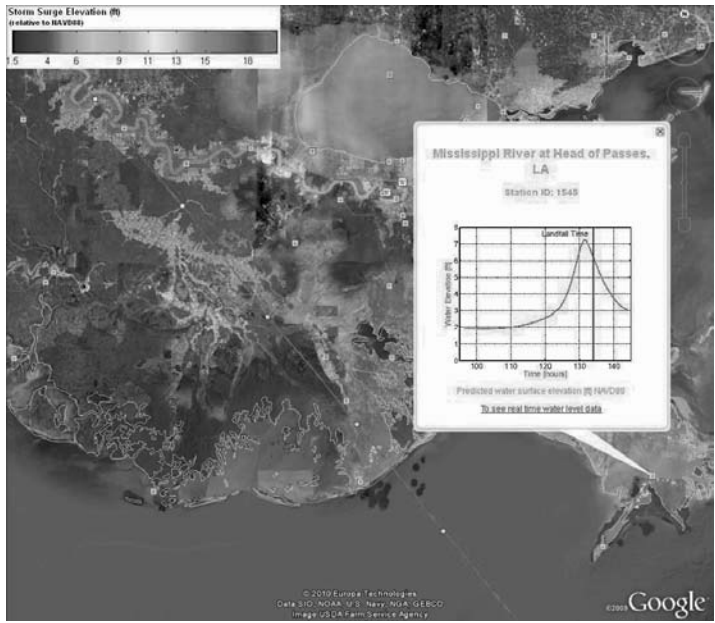


Figure 6. The forecasting results of Advisory number 27 displayed on the Google Earth. The color contour indicates the storm surge elevation; Green squares (■) on the map indicates the stations showing hydrographs (e.g., the white box shows a hydrograph at Mississippi River at Head of Passes)

DISCUSSION

An efficient method of forecasting storm surge using data mining has been developed. The RAT GUI operates on a regular PC and takes less than 5 minutes to predict high resolution local storm surge once advisory data are available at the NHC website. The RAT GUI has been successfully validated against historical hurricanes Camille and Katrina. Also the GUI has been demonstrated in real time for hurricane Gustav in order to identify the best matching synthetic storms which make the approach very efficient and robust. However, in order to improve the forecasting results, further scientific enhancements are required. In order to have smooth variations in synthetic hurricane tracks and major storm parameters, additional model runs and later populating the results into the database are necessary. With this robust database, the present RAT can be operational and useful to the emergency managers and planners. Using this RAT as a decision aid, the emergency personnel can quickly visualize high resolution local storm surge along the targeted coast. This will allow them to make quantitative and objective decisions by evaluating “what-if-scenarios” quickly after each advisory is issued and starting two to three days ahead of the landfall.

ACKNOWLEDGEMENTS

Authors acknowledge the Department of Homeland Security (DHS) for providing financial support. The research fund was provided through DHS Center for Natural Disasters, Coastal Infrastructure, and Emergency Management (NDCIEM) at Jackson State University (JSU). URS Corporation in Tallahassee, FL and Engineer Research and Development Center (ERDC) in Vicksburg, MS provided hurricane data and simulation results which were used in the RAT database. Drs. Donald Resio, Ty Wamsley and Bruce Ebersole of ERDC provided guidance during various phases of the project.

REFERENCES

- Fleming, J.G., C.W. Fulcher, R.A. Luettich, B.D. Estrade, G.D. Allen, and H.S. Winer (2007), “A real time storm surge forecasting system using ADCIRC”. Estuarine and Coastal Modeling Congress 2007, 893-912.
- Holland, G.J (1980), “An analytic model of the wind and pressure profiles in hurricanes”, *Monthly Weather Review*, 108(8):1212-1218.
- Mattocks, C. and C. Forbes (2008), “A real-time, event-triggered storm surge forecasting system for the state of North Carolina”, *Ocean Modeling*, 25:95-119.
- Niedoroda, A.W., D.T.Resio, G.R.Toro, D.Divoky, H.S.Das, and C.W.Reed (2010), “The role of wave set-up during extreme storms”, *Ocean Engineering*, 37: 82–90.
- Resio, D.T., S.J. Boc, L. Borgman, V. Cardone, A. Cox, W.R. Dally, R.G. Dean, D. Divoky, E. Hirsh, J.L. Irish, D. Levinson, A. Niedoroda, M.D. Powell, J.J. Ratcliff, V.Stutts, J. Suhada,

- G.R. Toro, and P.J. Vickery (2007), "White Paper on Estimating Hurricane Inundation Probabilities", Consulting Report prepared by USACE for FEMA.
- Rogers, W.E., J.M. Kaihatu, H.A. H. Petit, N. Booij, and L.H. Holthuijsen (2002), "Diffusion reduction in a arbitrary scale third generation wind wave model", *Ocean Engineering*, **29**:1357-1390.
- Thompson, E.F. and V.J. Cardone (1996), "Practical modeling of hurricane surface wind fields", *Journal of Waterway, Port, Coastal, and Ocean Engineering*, **122**(4):195-205.
- Westerink, J.J. and R.A. Luettich (1991), "Tide and storm surge predictions in the Gulf of Mexico using model ADCIRC-2D", Report to the U.S. Army Engineer Waterways Experiment Station, July, 1991.

EXPERIMENTAL STUDY OF SOLITARY WAVE INDUCED FLUID MOTIONS IN A SUBMERGED CAVITY

Ted Chu¹, Chih-Hua Chang² and Keh-Han Wang³

ABSTRACT

This paper presents an experimental investigation of solitary wave induced fluid motions in a submerged cavity. The evolution of the vortices and wave elevations were recorded for analysis. The tests were conducted in a glass-walled wave flume. A piston-typed wavemaker was installed on one end of the flume for generating desired solitary waves. A cavity of changeable size was positioned in the flume with two up-leveled acrylic panels. Three resistance-typed wave gauges were placed along the flume to record the wave profiles. The Planar Laser Induced Fluorescence (PLIF) technique was utilized to visualize and study the flow patterns as a solitary wave propagating past the cavity zone. The laser module used for the study had wavelength, output power, and projection fan angle of 532 nm (green light), 20 mW, and 100 degree, respectively. The laser excited the molecules of the fluorescent dyed fluid. As the incident wave passed by, any flow field feature would be illuminated. Each test was recorded with a video camera, and all the image frames could be further processed for comparison with the results obtained from a finite-analytic based two-dimensional (2-D) viscous flow model. This flow model solves combined stream function and vorticity equations. In terms of wave elevation and transformation of the formed vorticity, fairly good agreements are obtained between the numerical solutions and experimental observations. The results are presented and discussed.

Keywords: solitary wave propagation; cavity; PLIF; flow visualization

INTRODUCTION

Wave induced fluid motion as waves pass over a rectangular cavity (or trench) is known to cause a wider hydrodynamic or environmental impact on the natural or engineered systems. For example, the accumulated plankton, natural nutrients, sediments, or even contaminated materials in a submerged cavity are frequently disturbed by wave motions to allow the transport of the trapped materials to influence the surrounding ecological system. The induced vortex can also enhance the drift of sand to affect the navigational condition of waterways.

The early studies of wave and trench interaction problem were carried out by Lassiter (1972) using vertical matching conditions and by Lee and Ayer (1981) adopting the horizontal interface across a trench as the matching boundary. Later, Kirby and Dalrymple (1983) extended the solutions of Lee and Ayer (1981) to the cases with obliquely incident waves. Ting and Raichlen (1986) also employed Lee and Ayer's (1981) approach to analyze the wave induced velocity

¹ Department of Civil and Environmental Engineering, University of Houston, Houston, Texas 77204-4003, ytchu@uh.edu

² Department of Information Management, Ling-Tung University, Taichung, Taiwan 408, changbox@mail.ltu.edu.tw

³ Corresponding author: Department of Civil and Environmental Engineering, University of Houston, Houston, Texas 77204-4003, khwang@uh.edu

distribution in a trench. Recently, the damping effect for random waves propagating past a long trench was studied by Lee et al. (2009) to analyze the conditions of wave oscillation in harbors. Considering the non-Newtonian fluid conditions, Ting (1994) investigated wave interaction with fluid mud in a rectangular trench. Hsu et al. (2004) applied a RANS model to reveal the vortical flows due to a solitary wave propagating over two tandem trenches.

In this study, experiments for a solitary wave propagating past a submerged cavity were carried out to examine the transformation of wave profile and induced vortical motion in the cavity region. The recorded data in terms of the free-surface elevations and the evolutions of the fluid-particle motion around a submerged cavity are compared with the results obtained from a finite-analytic based 2D viscous flow model. The flow visualization showing the images of the emerging and the continuing development of the vortices inside the cavity are presented and discussed.

EXPERIMENTAL STUDY

This study was carried out with two phases of experimental measurements. The first phase emphasized on the transformation of the incident solitary wave as it propagated over a submerged cavity. Wave profiles showing the reflection and transmission process were recorded for the analysis. The second phase examined the fluid motion and the time evolution of the vortices inside the cavity zone. Flow visualization techniques were used to capture and analyze the flow patterns. The recorded data from both phases were used to verify the results of numerical simulations.

The undisturbed water depth ahead and beyond the cavity zone for all the test cases was set to 3 inches (7.62 cm). The total water depth of the cavity zone was 6 inches (15.24 cm) (7.62 cm of cavity depth plus 7.62cm of water above the cavity). Incident solitary waves with dimensionless wave heights of 0.42, 0.38, 0.27, and 0.14 were generated to create different incident wave conditions. Dimensionless cavity opening sizes of 1, 1.9, 3.5, and 5 were tested to provide insights to the effect of cavity opening on the propagation of incident waves and flow pattern within the cavity zone. All of the dimensionless variables mentioned above were obtained by normalizing the dimensional values with the undisturbed water depth.

Wave Flume

All the tests were carried out in a glass-walled wave flume, which had dimensions of 25 ft in length, 1 ft in width, and 3 ft in height. A piston-typed wavemaker was installed on one end of the flume. A 0.75 inch thick aluminum paddle was attached to the double carrier of the linear actuator of the wavemaker. The positions of the paddle could be prescribed through the control software to generate the desired incident wave conditions. On both ends of the flume, energy dissipating gravel beds were laid to minimize unwanted reflected waves traveling back into the study domain. Two sections of up-leveled acrylic made floor were placed in the flume to create the cavity. The size of the cavity opening was determined by the separation of the two sections of the acrylic floor.

To record the incident, reflected, and transmitted wave profiles, resistance-typed wave gauges were placed along the flume. Three wave gauges were utilized. The positions of the wavemaker, cavity, and wave gauges are shown in Figure 1.

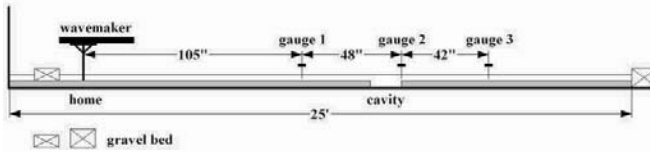


Figure 1. Schematic diagram of wave flume

Flow Visualization

The Planar Laser Induced Fluorescence (PLIF) technique was utilized to visualize and study the flow patterns as an incident solitary wave propagated over the cavity zone. A very thin laser sheet was generated and projected over the fluorescent dye filled cavity. The laser excited the fluorescent dye molecules. Any flow field feature would be illuminated as the incident wave passed over. Each test was recorded with a video camera, and selected image frames were further processed for comparison with the results obtained from numerical simulations. Figure 2 illustrates the flow visualization device configurations.

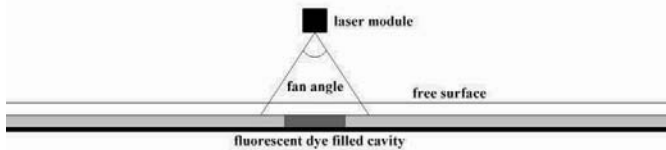


Figure 2. Set up of laser module for the use of PLIF technique

The laser module used for the study had a wavelength of 532 nm (green light). It had a set of optic lenses that generated a very thin sheet of laser. The thickness of the sheet could be adjusted by changing the focus of the lenses. The output power and projection fan angle of the module were 20 mW and 100 degree, respectively, which were adequate for the laser to penetrate the maximum water depth of 6 inches (free surface to bottom of cavity) and to cover the maximum cavity opening of 15 inches.

The fluorescent dye selected for the study was Rhodamine B, Basic Violet #10. Dye solutions with different concentrations were made and tested. It was found that mixing 0.003 grams of Rhodamine B with 1 liter of distilled water, 0.003 g/L, provided the optimal flow pattern visualization. In addition, a proper amount of NaCl was added to the dye solution in order to help the solution settle and stay in the cavity. Since the study was meant for single phase flow, the amount of NaCl added had to be controlled at its minimum level. 10 grams of NaCl was found to be the ideal amount.

The solution was injected into the cavity through a 15 gauge spinal needle, which was connected to a 1/8" diameter vinyl tubing. A clamp was used to control the injection of the dye